

## Positron production in heavy-ion collisions. II. Application of the formalism to the case of the U + U collision

T. Tomoda

*Max-Planck-Institut für Kernphysik, Heidelberg, West Germany*

(Received 28 December 1981)

The method developed in the preceding paper is applied to the calculation of the spectra of positrons produced in the U + U collision. Matrix elements of the radial derivative operator between adiabatic basis states are calculated in the monopole approximation, with the finite nuclear size taken into account. These matrix elements are then modified for the supercritical case with the use of the analytical method presented in paper I of this series. The coupled differential equations for the occupation amplitudes of the basis states are solved and the positron spectra are obtained for the U + U collision. It is shown that the decomposition of the production probability into a spontaneous and an induced part depends on the definition of the resonance state and cannot be given unambiguously. The results are compared with those obtained by Reinhardt *et al.*

### I. INTRODUCTION

In the first paper<sup>1</sup> of this series (hereafter referred to as I) we presented an analytical approach to treat the resonance which appears in the positron continuum during a collision between very heavy ions. We described a method to calculate matrix elements which appear in the coupled differential equations for the occupation amplitudes of the adiabatic single-particle states.

In the present paper the method developed in I is applied to the calculation of positron production in U + U collision. Although a calculation for this particular reaction has already been reported in Ref. 2, we believe that the present calculation, carried out along the lines of I, and a comparison with the results obtained previously, is useful in view of the very significant experimental effort that has been devoted to the measurement of positron spectra in heavy-ion collisions. As mentioned in I, the colliding nuclei are assumed to move on a classical trajectory, and the electron-electron interaction is neglected. The potential generated by two nuclei is approximated by its monopole part with the finite nuclear size taken into account.

In Sec. II the matrix elements appearing in the coupled differential equations are calculated. In Sec. III we solve the coupled differential equations for the collision of two <sup>238</sup>U nuclei. A brief summary is given in Sec. IV.

### II. CALCULATION OF THE MATRIX ELEMENTS

We calculate in this section the matrix elements of the operator  $i\partial/\partial t - H[R(t)]$  which appear in the coupled differential equations (I.2.10) [Eq. (2.10) of I] and (I.6.2) for the occupation amplitudes of the adiabatic single-particle states. First, the time-independent Dirac equation (I.2.6) for fixed internuclear distance  $R$  must be solved. Since we adopt the monopole potential (I.2.5), which is generated by uniformly charged spheres of a radius  $R_n = r_0 A^{1/3}$  with  $r_0 = 1.2$  fm, analytical solutions are known for both the regions  $r < R_-$  (Ref. 3) and  $r > R_+$  (Ref. 4), where  $R_{\pm} = R \pm R_n$ . (The subscript  $i$  is omitted because only symmetric projectile-target combinations are considered in the present paper.) For the intermediate region  $R_- < r < R_+$ , the Dirac equation is solved numerically and the solution is matched to the inner and outer analytical solutions which satisfy appropriate boundary conditions. In this manner we obtain bound-state energies  $E_n(R)$ , and continuum and bound-state wave functions. The normalization (I.2.7) of the continuum wave functions is obtained via the knowledge<sup>4</sup> of the asymptotic property of the outer solutions. In order to normalize the bound-state wave functions we use the equation

$$\frac{dE_n}{dR} = \left\langle \varphi_n \left| \frac{\partial V}{\partial R} \right| \varphi_n \right\rangle, \quad (2.1)$$

which holds for a normalized wave function  $\varphi_n$ . It is shown below that the use of Eq. (2.1) enables us to normalize  $\varphi_n$  by carrying out a numerical integration only for the intermediate region  $R_- < r < R_+$ . For the supercritical case ( $R < R_{cr}$ ), the energy  $E_0$  and the width  $\Gamma(E_0, E_0)$  of the resonance in the positron continuum must be calculated. These are obtained by fitting the energy dependence of the normalization factor for the inner part ( $r < R_-$ ) of the wave function in the energy range  $E_0 - \Gamma \lesssim E_- \lesssim E_0 + \Gamma$  in terms of the square root of a Lorentzian function. Figure 1 shows the binding energies of the lowest eight  $s_{1/2}$  and  $p_{1/2}$  states calculated for the U + U system. It is seen that their  $R$  dependence can be well described by a power<sup>5</sup> of  $R$  for  $R \lesssim 300$  fm except for the  $2p_{1/2}$  state, for which the deviation is rather large. The  $1s_{1/2}$  state becomes a resonance in the positron continuum for  $R < R_{cr} = 32.6$  fm.

In order to obtain matrix elements of the radial derivative operator  $\partial/\partial R$ , we evaluate the integral (I.7.2). Since the integration up to  $r = R_-$  can be done analytically, the numerical integration is carried out only for the intermediate region  $R_- < r < R_+$ . For the supercritical case  $R < R_{cr}$ , we have to evaluate also matrix elements which involve the resonance state  $\varphi_r$  and/or the modified positron continuum state  $\chi_{E_-}$ . The evaluation of

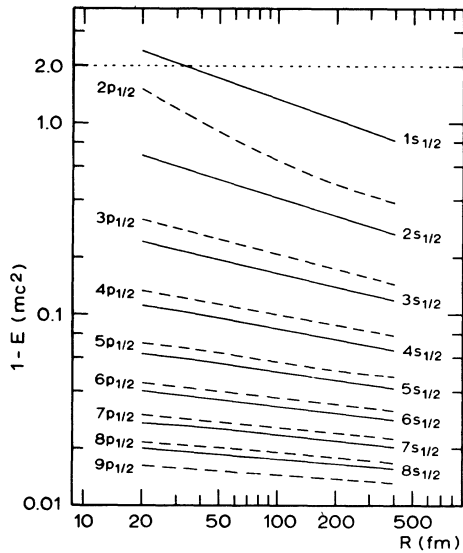


FIG. 1. Binding energies,  $1 - E_n$ , of the lowest eight  $s_{1/2}$  and  $p_{1/2}$  states as functions of internuclear distance  $R$  between two  $^{238}\text{U}$  nuclei calculated in the monopole approximation. A uniformly charged sphere is assumed for the charge distribution of uranium.

these matrix elements proceeds in the following way. We first choose a penetrability  $P(E_-)$  of the form [see (I.4.12)]

$$P(E_-) = P^{(0)}(E_-)(-E_- - 1)^{-n} \quad (n \geq 2), \quad (2.2)$$

where  $P^{(0)}(E_-)$  is the WKB penetrability<sup>6</sup> (I.4.10), and then obtain the reduced width  $\gamma(E_0)$  from the equation

$$\gamma(E_0) = \Gamma(E_0, E_0) / P(E_0). \quad (2.3)$$

The product  $P(E_-)\gamma(E_0)$  gives the width  $\Gamma(E_-, E_0)$  and accordingly determines the weight function  $a_{E_-}$ , Eq. (I.5.4). Figure 2 shows the reduced width for different values of  $n$  as a function of the resonance energy. Values corresponding to  $n = 2$  and 4 are used in the following. The dashed line with  $n = 0$  is shown to demonstrate that the reduced width corresponding to the WKB penetrability is approximately given by  $\gamma^{(0)}(E_0) \approx 0.45 |E_0|$  [see Eq. (I.4.11)].

As discussed in I, the derivative of the width

$$\frac{d\Gamma(E_-, E_0)}{dE_-} = \gamma(E_0) \frac{dP(E_-)}{dE_-}, \quad (2.4)$$

gives the order of magnitude of the error associated with the approximation made in evaluating the matrix elements which involve  $\varphi_r$  and/or  $\chi_{E_-}$ . In Table I are listed some values of  $d\Gamma(E_-, E_0)/dE_-$  for the resonance energy  $E_0 = -1.6$  ( $R \approx 16$  fm), and for  $n = 2$  and 4. We see that the overall trend is better for the case of  $n = 2$  and the derivative is mostly less than 1% even for  $n = 4$ . It should be

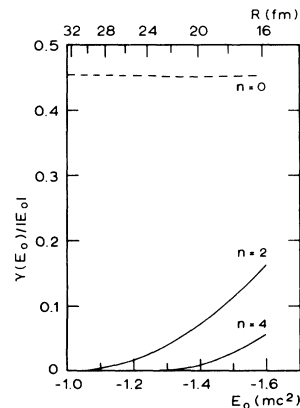


FIG. 2. Calculated reduced width of the  $1s_{1/2}$  resonance for the U + U system as a function of the resonance energy  $E_0$ . The three lines correspond to different values of  $n$  in the definition of the penetrability (2.2). The values with  $n = 2$  and 4 are used in the calculation.

TABLE I.  $d\Gamma(E_-, E_0)/dE_-$  for the resonance energy  $E_0 = -1.6$  ( $R \approx 16$  fm) and for the U + U system. See Eqs. (2.2)–(2.4).

$E_-$ ( $mc^2$ )	$d\Gamma/dE_-$ ( $n=2$ )	$d\Gamma/dE_-$ ( $n=4$ )
-1.1	-0.0008	-0.0200
-1.2	-0.0081	-0.0342
-1.4	-0.0105	0.0061
-1.6	-0.0041	0.0095
-1.8	-0.0001	0.0062
-2	0.0016	0.0036
-3	0.0015	0.0003
-4	0.0007	0.0001

stressed that the values listed here correspond to the worst case for the U + U system. They fall off according to  $\sim |E_0|(|E_0| - 1)^n$  as  $|E_0|$  decreases (i.e.,  $R$  increases) because of the presence of the factor  $\gamma(E_0)$  in Eq. (2.4).

Figure 3 shows the matrix element  $V_{E_-}$ , Eq. (I.5.7), which causes the spontaneous decay of the positron resonance state, calculated for  $R=16$  and 24 fm and  $n=2$  and 4. It is noted that (1)  $V_{E_-}$  depends significantly on the choice of  $n$  although it has a unique value  $-\Gamma(E_0, E_0)/2\pi]^{1/2}$  at the resonance energy [ $E_0(16 \text{ fm}) = -1.59$ ,  $E_0(24 \text{ fm}) = -1.24$ ]; (2) the dependence on  $E_-$  is given by  $[P(E_-)]^{1/2}$ , so that the shape of the curve does not change with  $R$ ; (3)  $V_{E_-}$  has a sharp cutoff at  $E_c$ , with a value of  $E_c$  chosen to be  $-2.1$  unless specified otherwise. The latter two features distinguish our  $V_{E_-}$  from the corresponding matrix element of Ref. 2.

Using  $V_{E_-}$  obtained above and Eq. (I.7.21), we

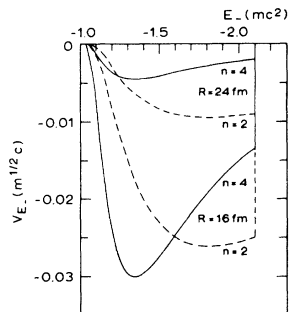


FIG. 3. Matrix elements  $V_{E_-} = \langle \varphi_r | H(R) | \chi_{E_-} \rangle$ , Eq. (I.5.7), with the cutoff energy  $E_c = -2.1$ , as functions of  $E_-$  for different internuclear distances and different values of the power  $n$  in the definition of the penetrability.

can calculate the matrix elements of  $\partial/\partial R$  which involve the basis states  $\varphi_r$  and/or  $\chi_{E_-}$ , Eqs. (I.7.9), (I.7.13), (I.7.16), and (I.7.20). Figure 4 shows the matrix elements  $\langle \chi_{E_-} | \partial/\partial R | \varphi_r \rangle$ , Eq. (I.7.9), which are responsible for the induced decay of the positron resonance. As can be seen from the figure, these matrix elements depend on the value of  $n$ . While for  $n=4$  they are continuous at  $R=R_{cr}$ , those for  $n=2$  are not [see the discussion below Eq. (I.7.12)], and smaller than the former by a factor 3–20 in the supercritical region  $R < R_{cr}$ . There appears a singularity due to  $\mathcal{P}/[E_0(R) - E_-]$ , cf. Eq. (I.7.9). This singularity does not, however contribute to the solutions of the coupled differential equations (I.6.2) because it is multiplied by slowly changing factors: (1) the phase factor  $\exp[i(\theta_{E_-} - \theta_0)]$  becomes stationary; (2) the relative change of the amplitude  $c_0$ ,  $|c_0|^{-1} dc_0/dR$ , does not exceed  $\approx 0.03 \text{ fm}^{-1}$  in practical applications (see the example described in Sec. IV); (3) the same holds also for the amplitude  $c_{E_-}$ . Consequently we can use approximate matrix elements which are smoothly interpolated across the principal-value singularity.

Figure 5 shows the matrix elements

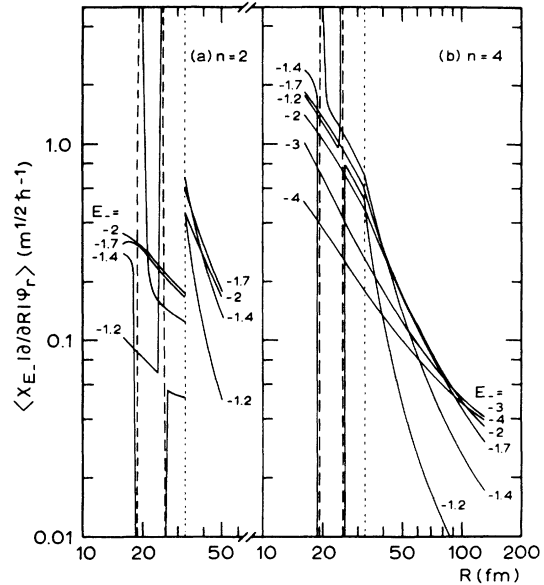


FIG. 4. Matrix elements  $\langle \chi_{E_-} | \partial/\partial R | \varphi_r \rangle$ , Eq. (I.7.9), with  $E_c = -2.1$  as functions of  $R$  for (a)  $n=2$  and (b)  $n=4$ . For  $E_- < E_c$ , these are equal to  $\langle \varphi_{E_-} | \partial/\partial R | \varphi_r \rangle$  of Eq. (I.7.16) and do not depend on  $n$  in the present approximation. The dashed lines indicate negative values and the dotted lines the critical internuclear distance  $R_{cr} = 32.6$  fm.

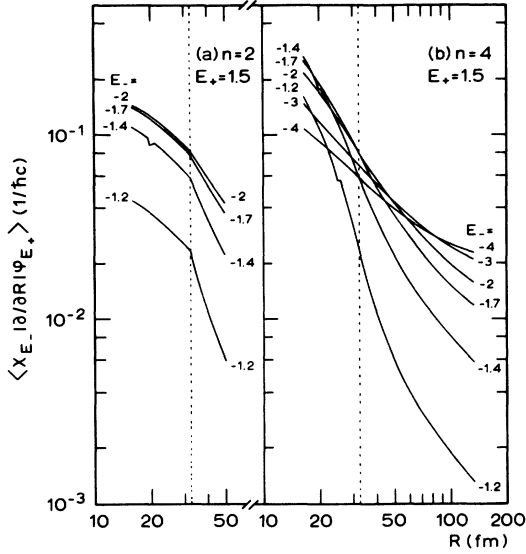


FIG. 5. Matrix elements  $\langle \chi_{E_-} | \partial/\partial R | \varphi_{E_+} \rangle$ , Eq. (I.7.20), with  $E_+ = 1.5$  and  $E_c = -2.1$  for (a)  $n=2$  and (b)  $n=4$ . For  $E_- < E_c$ , these are equal to the unmodified matrix elements  $\langle \varphi_{E_-} | \partial/\partial R | \varphi_{E_+} \rangle$ . It is apparent that the latter do not depend on  $n$ . The dotted lines indicate  $R_{cr}$ .

$\langle \chi_{E_-} | \partial/\partial R | \varphi_{E_+} \rangle$ , Eq. (I.7.20), with  $E_+ = 1.5$  for (a)  $n=2$  and (b)  $n=4$ . Both of them are continuous at  $R=R_{cr}$  in contrast with those of Fig. 4. It is noted that here, too, the matrix elements with  $n=2$  are smaller than those with  $n=4$  in the region  $R < R_{cr}$ . Small dips at the internuclear distance where  $E_0(R)$  becomes equal to  $E_-$  are due to approximations made in evaluating the first term in the square bracket in Eq. (I.7.20).

### III. POSITRON PRODUCTION IN U + U COLLISION

In this section we calculate the positron production probability for a head-on collision of two  $^{238}\text{U}$  nuclei with a laboratory projectile energy  $E/A = 5.9$  MeV. For  $R(t)$ , we use a Rutherford trajectory. In order to suppress the well-known spurious coupling<sup>7</sup> in the asymptotic region, all the matrix elements of  $\partial/\partial R$  for  $R > 1500$  fm are multiplied by a Gaussian damping factor  $\exp\{-[(R - 1500 \text{ fm})/750 \text{ fm}]^2\}$  as in Ref. 2.

#### A. Spontaneous and induced decay of the $1s_{1/2}$ resonance

It was explained in I that the decomposition of the reaction amplitude into a “spontaneous” and an

“induced” part is ambiguous and depends on the choice of the resonance wave function. To demonstrate this ambiguity, let us consider a positron production process assuming that there was initially a hole in the  $1s_{1/2}$  state. We solve the equations for the occupation amplitudes, Eqs. (I.2.10) and (I.6.2), in first-order perturbation, which is adequate for this situation. Putting the zeroth-order amplitudes

$$\begin{aligned} c_{1s,0}^{(0)}(t) &= 1, \\ c_{1s,E_-}^{(0)}(t) &= 0, \end{aligned} \quad (3.1)$$

into the right-hand side of Eqs. (I.2.10) and (I.6.2), we obtain the first-order solution

$$\begin{aligned} c_{1s,E_-}^{(1)}(+\infty) &= - \int_{-\infty}^{+\infty} dt (\langle \chi_{E_-} | \dot{\varphi}_r \rangle + iV_{E_-}^*) \\ &\quad \times \exp[i(\theta_{E_-} - \theta_0)], \end{aligned} \quad (3.2)$$

where the sum in the parentheses should read  $\langle \varphi_{E_-} | \dot{\varphi}_r \rangle$  for  $R(t) > R_{cr}$ . Since  $\langle \chi_{E_-} | \dot{\varphi}_r \rangle$  ( $\langle \varphi_{E_-} | \dot{\varphi}_r \rangle$ ) and  $V_{E_-}$  are odd and even real functions of time, respectively, each contribution to the integral is purely imaginary [see also Eq. (I.2.9)]. Figure 6 shows  $\text{Im } c_{1s,E_-}^{(1)}(+\infty)$  for  $n=2$  and 4. The components labeled “induced” and “spontaneous” correspond to the contributions which come from the first and second term in the parentheses in Eq. (3.2). It can be seen from the figure that this decomposition depends strongly on the value of  $n$ ,

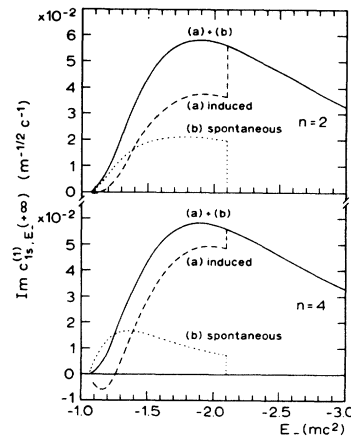


FIG. 6. Imaginary part of the production amplitude for a positron of energy  $E_-$  emitted in a head-on collision of U + U with  $E/A = 5.9$  MeV, and evaluated using a first-order perturbation calculation with  $E_c = -2.1$ , assuming an initial hole in the  $1s_{1/2}$  state. The solid lines give the full amplitude, the square of which yields the positron spectrum.

while the total amplitudes coincide with each other very well. (The difference between the two total amplitudes is 1% at  $E_- = -1.2$  and only 0.1% at  $E_- = -2$ . These values should be compared with the values of  $d\Gamma/dE_-$  listed in Table I. They are  $\leq 3\%$  for  $E_- = -1.2$  and  $\leq 0.4\%$  for  $E_- = -2$ .) This shows that no physical meaning can be attached to the above-mentioned decomposition in a heavy-ion collision.

Table II shows the dependence of the positron production amplitude on the cutoff energy  $E_c$  [see Eq. (I.4.3)]. For the cases  $E_c > E_-$ , the corresponding amplitudes are calculated by using only the matrix element  $\langle \varphi_{E_-} | \hat{\varphi}_r \rangle$  without introducing either the modified continuum state  $\chi_{E_-}$  or the spontaneous coupling  $V_{E_-}$ . We note from the table that the dependence on  $E_c$  is very weak ( $\sim 1\%$  for  $E_- = -2$ ).

Lastly, a comparison can be made between those contributions to the integral (3.2) which come from  $R(t) > R_{cr}$  and  $R(t) < R_{cr}$ . These are about the same for  $-1.5 \gtrsim E_- \gtrsim -2.5$  within a maximum difference of  $\sim 20\%$ .

### B. Solution of the full coupled differential equations

In this section the full coupled differential equations (I.2.10) and (I.6.2) are solved for the  $s_{1/2}(\kappa = -1)$  and  $p_{1/2}(\kappa = 1)$  channels which give the most important contributions in the collision under consideration. Neglecting the coupling among positron continuum states which is about 2 orders of magnitude smaller than that among the electron continuum states, we take for each channel ( $\kappa = \pm 1$ ) one positron continuum state of energy  $E_-$ , the lowest eight bound states up to  $8s_{1/2}$  or  $9p_{1/2}$  and twelve discretized electron continuum states up to  $E_+ = 4$  which are equally spaced. We solve the coupled differential equations with the ini-

TABLE II. Dependence of the positron production amplitude on the cutoff energy  $E_c$ . The values calculated for  $E_- = -2$  and  $-4$  with  $n=2$  are listed.

$E_c$ ( $mc^2$ )	$\text{Im}c_{1s, E_-}^{(1)}(+\infty)(m^{-1/2}c^{-1})$	
	$E_- = -2$	$E_- = -4$
-1.9	0.0571	0.0149
-2.1	0.0577	0.0149
-4.1	0.0577	0.0152

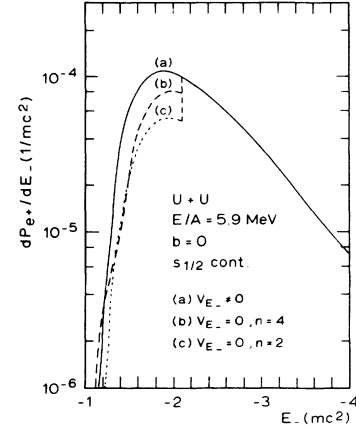


FIG. 7. Positron production probability for a head-on collision of two  $^{238}\text{U}$  with  $E/A = 5.9$  MeV. Initially filled bound states up to  $3s_{1/2}$  were assumed and the full coupled differential equations for the  $s_{1/2}$  channel were solved.

tial condition

$$c_{E_-, E}(-\infty) = \delta_{E_-, E}, \quad (3.3)$$

and calculate the positron production probability  $dP_{e^+}/dE_-$  according to Eq. (I.6.5) after multiplication by a spin degeneracy factor of 2. The lowest three bound states for each channel up to  $3s_{1/2}$  (or  $4p_{1/2}$ , respectively) are assumed to be filled initially.<sup>2</sup> Figure 7 shows the result of the calculation for the  $s_{1/2}$  channel for the head-on collision of two  $^{238}\text{U}$  nuclei with  $E/A = 5.9$  MeV. Curve *a* includes the contributions from the derivative matrix elements and  $V_{E_-}$  coherently, and the results of the calculation with  $n=2$  and 4 agree very well with each other: They differ by not more than 0.25% at  $E_- \approx -2$ . This gives us confidence in the accuracy of our approximation scheme. On the other hand, if we switch off the coupling matrix element  $V_{E_-}$  which is responsible for the spontaneous decay of the  $1s_{1/2}$  resonance, we obtain the curves *b* or *c*

TABLE III. Dependence of the positron production probability on the cutoff energy  $E_c$ . The  $s_{1/2}$  channel contributions calculated with  $n=2$  are listed.

$E_c$ ( $mc^2$ )	$dP_{e^+}/dE_- (1/mc^2)$	
	$E_- = -2$	$E_- = -4$
-1.9	$1.042 \times 10^{-4}$	$7.07 \times 10^{-6}$
-2.1	$1.061 \times 10^{-4}$	$7.07 \times 10^{-6}$
-4.1	$1.061 \times 10^{-4}$	$7.30 \times 10^{-6}$

TABLE IV. Positron production probability for  $E_- = -2$  calculated perturbatively. The  $s_{1/2}$  channel contributions are listed. The values in the second and third lines are obtained by including only the specified intermediate states.

	$dP_{e^+}/dE_-  _{E_-=-2} (10^{-4}/mc^2)$	
	$n=2$	$n=4$
First order	0.36	0.78
First and second (1s)	0.22	0.22
First and second (1s,2s,3s)	2.37	3.41
First and second (all)	5.51	9.32
Full calculation	1.061	1.058

which depend considerably on the value of  $n$ . This again demonstrates the ambiguity of the decomposition of the amplitude. It should be noted that the positron spectrum of Fig. 7 curve *a* has almost the same shape as the squared amplitude obtained in the Sec. III A. Multiplying the latter by a normalization factor 0.032, which is about one-fourth of the calculated  $1s_{1/2}$  hole creation probability 0.12, we find that these two spectra coincide with each other within an accuracy of  $\pm 2\%$  for the main part  $-1.4 \gtrsim E_- \gtrsim -4$  of the spectra.

The cutoff energy  $E_c$  was chosen to be  $-2.1$  for the above calculation. The dependence of the results on  $E_c$  is very weak for the present case, too. As can be seen from Table III, the positron production probability changes by  $\sim 2\%$  for  $E_- = -2$  according to whether  $E_c$  is smaller or larger than  $E_-$ .

We now compare the above results with those of perturbative calculations. Putting the zeroth-order amplitude

$$c_{E_-,E}^{(0)}(t) = \delta_{E_-,E}, \quad (3.4)$$

into the right-hand side of Eqs. (I.2.10) and (I.6.2), we obtain the first-order amplitudes  $c_{E_-,E}^{(1)}(t)$  as a result of integration. Substitution of the obtained  $c_{E_-,E}^{(1)}(t)$  into the right-hand side of the coupled equations then yields the second-order amplitudes  $c_{E_-,E}^{(2)}(t)$ . Table IV lists the results of first- and second-order calculations together with those of the full calculation above. First of all we note that the results of the perturbation calculation depend on the value of  $n$ . This is because the modified positron continuum state  $\chi_{E_-}$  depends on  $n$  so that the zeroth-order solution is different for different  $n$ . The production probability increases drastically as we include more and more intermediate states in the second-order calculation. It is seen that a simple perturbative picture does not apply.

Figure 8 shows the sum of the  $s_{1/2}$  and  $p_{1/2}$  contributions to the positron spectra in head-on collisions of  $^{238}\text{U} + ^{238}\text{U}$  and  $^{208}\text{Pb} + ^{208}\text{Pb}$  with  $E/A = 5.9$  MeV. In order to compare these results with those of Ref. 2, calculations were performed with four more electron continuum states which double the number of states between  $1 < E_+ < 2$ . This gives about 3% and 4% increase of  $dP_{e^+}/dE_-$  at  $E_- = -2$  for Pb + Pb and U + U, respectively. While the value for the Pb + Pb collision coincides with that of Ref. 2, the value for the U + U collision is about 8% smaller than the corresponding value of Ref. 2.

#### IV. SUMMARY

We have applied the formalism developed in I to the problem of positron production in the U + U

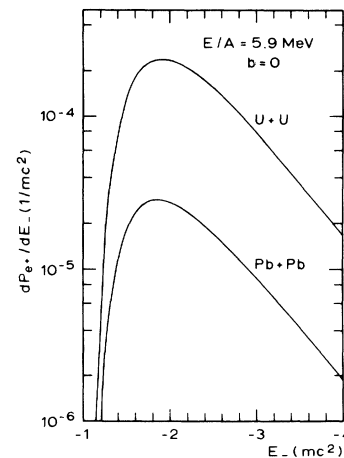


FIG. 8. Positron production probability for head-on collisions of  $^{238}\text{U} + ^{238}\text{U}$  and  $^{208}\text{Pb} + ^{208}\text{Pb}$  with  $E/A = 5.9$  MeV. Initially filled bound states up to  $3s_{1/2}$  and  $4p_{1/2}$  were assumed and the full coupled differential equations for the  $s_{1/2}$  and  $p_{1/2}$  channels were solved.

collision. It was found that the analytical method to calculate the matrix elements is quite effective and simplifies the numerical calculations considerably. The errors associated with the approximations made in the analytical manipulations are under good control and estimated to be of the order of 1%. These matrix elements were used in solving the coupled differential equations for the occupation amplitudes of adiabatic basis states. It was demonstrated that the decomposition of the production probability into a spontaneous and an induced part depends on the definition of the resonance state and cannot be given unambiguously. The present calculations were compared with those of Ref. 2.

While the results for the undercritical system  $Pb + Pb$  agree with each other very well, the present result for the supercritical system  $U + U$  is about 8% smaller than the corresponding value of Ref. 2. This might help us understand the absolute values observed in experiments,<sup>8,9</sup> which are consistently smaller than those calculated in Ref. 2.

#### ACKNOWLEDGMENTS

I am grateful to Professor H. A. Weidenmüller for valuable discussions and for his critical reading of the manuscript. I acknowledge the Max-Planck-Gesellschaft for financial support.

<sup>1</sup>T. Tomoda and H. A. Weidenmüller, *Phys. Rev. A* **26**, 162 (1982), paper I.

<sup>2</sup>J. Reinhardt, thesis, Universität Frankfurt, 1979 (unpublished); J. Reinhardt, G. Soff, B. Müller, and W. Greiner, *Prog. Part. Nucl. Phys.* **4**, 547 (1980); J. Reinhardt, B. Müller, and W. Greiner, *Phys. Rev. A* **24**, 103 (1981).

<sup>3</sup>A. Messiah, *Quantum Mechanics* (North-Holland, Amsterdam, 1962).

<sup>4</sup>B. Müller, J. Rafelski, and W. Greiner, *Z. Phys.* **257**, 183 (1972).

<sup>5</sup>G. Soff, J. Reinhardt, and W. Betz, *Phys. Scr.* **17**, 417 (1978).

<sup>6</sup>V. S. Popov, V. L. Eletsy, V. D. Mur, and D. N. Voskresensky, *Phys. Lett.* **80B**, 68 (1978); V. S. Popov, D. N. Voskresenskii, V. L. Eletsy, and V. D. Mur, *Zh. Eksp. Teor. Fiz.* **76**, 431 (1979) [*Sov. Phys.—JETP* **49**, 218 (1979)].

<sup>7</sup>D. R. Bates and R. McCarroll, *Proc. R. Soc. London Ser. A* **245**, 175 (1958).

<sup>8</sup>H. Backe, L. Handschug, F. Hessberger, E. Kankleit, L. Richter, F. Weik, R. Willwater, H. Bokemeyer, P. Vincent, Y. Nakayama, and J. S. Greenberg, *Phys. Rev. Lett.* **40**, 1443 (1978); C. Kozhuharov, P. Kienle, E. Berdermann, H. Bokemeyer, J. S. Greenberg, Y. Nakayama, P. Vincent, H. Backe, L. Handschug, and E. Kankleit, *ibid.* **42**, 376 (1979); H. Backe, W. Bonin, W. Engelhardt, E. Kankleit, M. Mutterer, P. Senger, F. Weik, R. Willwater, V. Metag, and J. B. Wilhelmy, GSI Scientific Report, 1979 (Darmstadt, 1980), p. 101.

<sup>9</sup>E. Berdermann, F. Bosch, M. Clemente, F. Güttner, P. Kienle, W. Koenig, C. Kozhuharov, B. Martin, B. Povh, H. Tsertos, W. Wagner, and Th. Walcher, GSI Scientific Report, 1980 (Darmstadt, 1981), p. 128; H. Bokemeyer, H. Folger, H. Grein, S. Ito, D. Schwalm, P. Vincent, K. Bethge, A. Gruppe, R. Schulé, M. Waldschmidt, J. S. Greenberg, J. Schwappe, and N. Trautmann, *ibid.*, p. 127.